SCIENCE CHINA
Chemistry

• ARTICLES •

July 2015 Vol.58 No.7: 1144–1151
doi: 10.1007/s11426-015-5411-0

New triphenylamine-based sensitizers bearing double anchoring units for dye-sensitized solar cells

Jie Shi[1,2], Zhaofei Chai[1], Runli Tang[1], Jianli Hua[3], Qianqian Li[1*] & Zhen Li[1*]

[1]*Hubei Key Lab on Organic and Polymeric Opto-Electronic Materials; Department of Chemistry, Wuhan University, Wuhan 430072, China*
[2]*Hubei Key Laboratory of Oilcrops Lipid Chemistry and Nutrition; Oil Crops Research Institute, Chinese Academy of Agricultural Sciences, Wuhan 430062, China*
[3]*Key Laboratory for Advanced Materials and Institute of Fine Chemicals; East China University of Science & Technology, Shanghai 200237, China*

Received September 22, 2014; accepted October 20, 2014; published online May 4, 2015

Two organic sensitizers (**LI-33** and **LI-34**) with double anchoring units were synthesized and utilized for dye sensitized solar cells (DSSCs), which contained thiophene or vinyl thiophene as π-bridge. The introduction of double anchoring units can change their absorption spectra and energy levels in a large degree, thus, the better light-harvesting ability and the convenient electron transfer along the whole molecule can be obtained. The solar cell based on **LI-34** exhibited a broad incident photon-to-current conversion efficiency (IPCE) spectrum and high conversion efficiency (η=6.05%) with coadsorbent CDCA.

organic sensitizers, **double anchoring units**, **dye-sensitized solar cells**, **triphenylamine**

1 Introduction

The intense research on various light-harvesting devices has emerged rapidly, since the ever-increasing demands for renewable energy sources. Recently, dye-sensitized solar cells (DSSCs), as a new kind of photovoltaic devices, have attracted considerable attention due to their low cost, ease of production and flexibility in comparison with crystalline silicon [1,2]. In DSSCs, sensitizer is the key component, which is like the light harvesting antennae, and plays an important role in efficient light harvesting and electron generation/transfer. Thus, it is necessary to design and synthesize dye sensitizers with novel structures to optimize their photovoltaic performance.

So far, ruthenium bipyridyl and zinc porphyrin complexes hold the record in DSSCs. In addition, much research interest has been focused on metal-free organic dyes for the abundant raw materials and the tailorable molecular structures [5–10]. Most common investigated structure of organic sensitizers is the type of donor-π-acceptor—the acceptor group carries an anchoring group, such as carboxylic acid to the TiO_2 surface [11–18]. During photoexcitation, an intramolecular charge transfer takes place from electron donor to acceptor, from where the photoelectron can be injected into the conduction band of TiO_2 [19].

Anchoring groups, which also act as the acceptor, play an important role in electron injection, and are critical to the conversion efficiency of the whole molecule. But only a few literatures reported the sensitizers with non-single anchoring units [20]. In this paper, two organic dyes with double electron acceptors (cyanoacetic acid) were synthesized and characterized (**LI-33** and **LI-34**, Scheme 1), and further applied as sensitizers in DSSCs. Dyes with two anchoring group would afford more chance for the injection of electron into TiO_2 electrode. The thiophene or vinyl thiophene group was selected as a conjugation bridge. In addition, to reduce the possible intermolecular π-π stacking, 4-*tert*-

*Corresponding authors (email: qianqian-alinda@163.com; lizhen@whu.edu.cn or lichemlab@163.com)

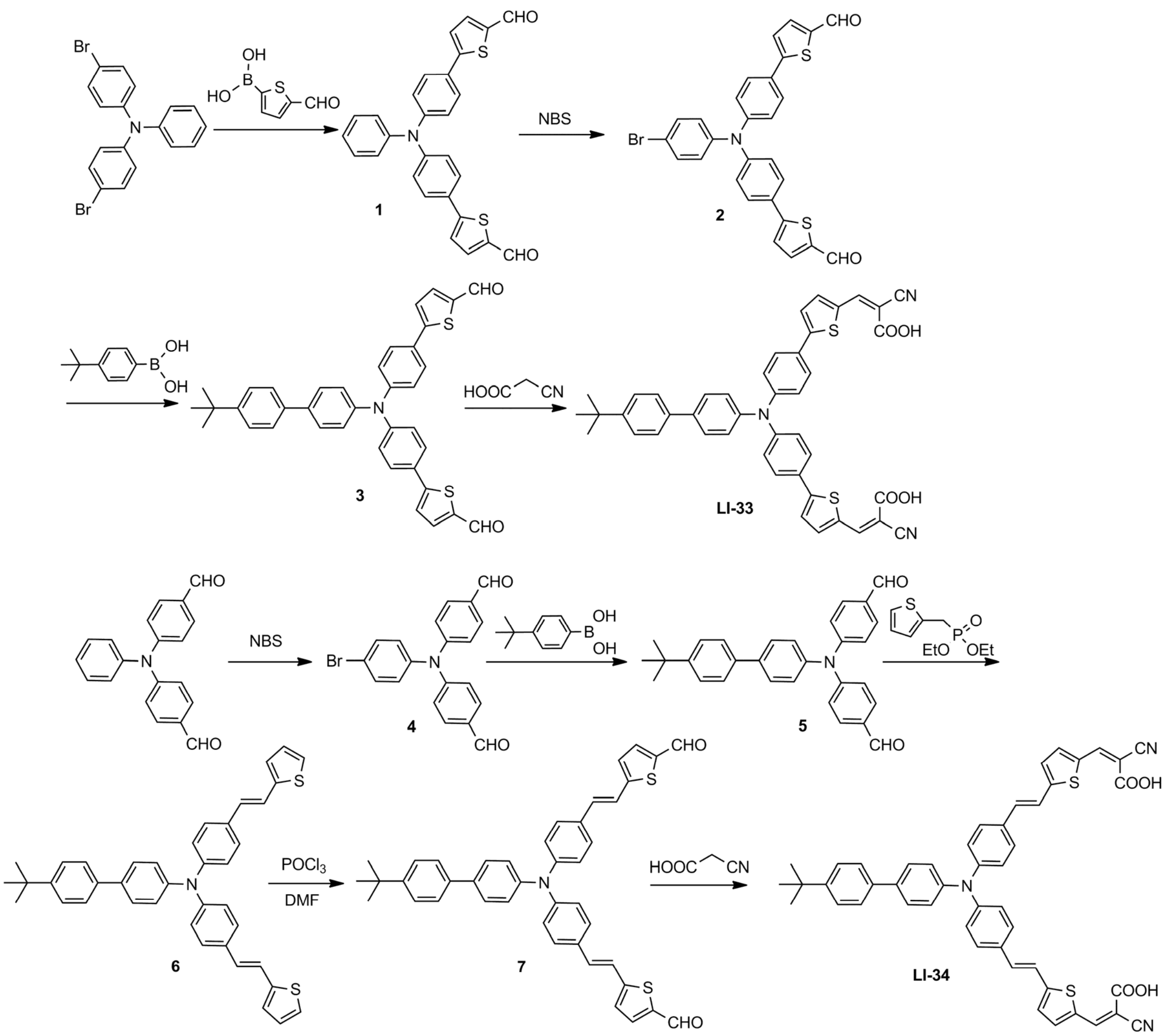

Scheme 1 Synthetic route of **LI-33** and **LI-34**.

butylbenzene moiety was chosen as an anti-aggregation group, which was linked to the triphenylamine (TPA) unit. Herein, we reported the detailed syntheses, structural characterizations, electrochemical characters, theoretical calculations, and their conversion efficiencies.

2 Experimental

2.1 Materials

Under an atmosphere of dry nitrogen, tetrahydrofuran (THF) and toluene were dried over, and distilled from K-Na alloy. *N*,*N*-dimethylformamide (DMF) was distilled from CaH_2 with the similar procedures. After the addition of phosphorus pentoxide, 1,2-dichloromethane was dried over and distilled. Before use, phosphorus oxychloride was freshly distilled. All reagents were purchased, and used as received. 4-Bromo-*N*-(4-bromophenyl)-*N*-phenylaniline and 4,4'-(phenylazanediyl)dibenzaldehyde were prepared following the literatures [21,22].

2.2 Instrumentation

A Varian Mercury 300 spectrometer (USA) conducted ^{1}H and ^{13}C NMR spectroscopy study with using tetramethylsilane (TMS, δ=0 ppm) as internal standard. A Shimadzu UV-2550 spectrometer (Japan) was used to obtain UV-visible spectra. Cyclic voltammograms were carried out on a CHI 660 voltammetric analyzer at room temperature with nitrogen-purged anhydrous dichloromethane as the solvent. Tetrabutylammonium hexafluorophosphate ($TBAPF_6$) acted as the supporting electrolyte, a platinum disk was used as the working electrode, and an Ag/AgCl electrode was used as the quasi-reference electrode. The ferrocene/ferrocenium redox couple was applied for potential calibration. The scanning rate was 100 mV/s. MALDI-TOF-MS spectra were recorded with Voyager-DE-STR MALDI-TOF (ABI, USA).

2.3 Synthesis

2.3.1 5,5'-(4,4'-(Phenylazanediyl)bis(4,1-phenylene))dithiophene-2-carbaldehyde (**1**)

4-Bromo-*N*-(4-bromophenyl)-*N*-phenylaniline (1.0 mmol, 0.40 g), 5-formylthiophen-2-yl boronic acid (2.5 mmol, 0.39 g), and sodium carbonate (10.0 mmol, 1.06 g) were mixed. After degassed and charged with nitrogen, $Pd(PPh_3)_4$ (10 mg) was added, the solution of THF and water (2:1) was injected into the mixture. The reaction was refluxed at 80 °C for 24 h, then, cooled to room temperature. The organic layer was separated, and dried over anhydrous sodium sulfate. Compound **1** was purified by column chromatography over silica gel as a yellow solid (0.47 g, 35%). ^{1}H NMR ($CDCl_3$, 300 MHz) δ (ppm): 9.95 (s, 1H, –CHO), 9.86 (s, 1H, –CHO), 7.78–7.71 (m, 2H, ArH), 7.53 (d, *J*=8.4 Hz, 2H, ArH), 7.40–7.31 (m, 5H, ArH), 7.26–7.21 (m, 6H, ArH), 7.05 (d, *J*=8.7 Hz, 2H, ArH), 6.98 (d, *J*=8.4 Hz, 2H, ArH).

2.3.2 5,5'-(4,4'-(4-Bromophenylazanediyl)bis(4,1-phenylene)) dithiophene-2-carbaldehyde (**2**)

After compound **1** (1.3 mmol, 0.81 g) was dissolved in $CHCl_3$ (15 mL), *N*-bromosuccinimide (1.5 mmol, 0.27 g) was added slowly, then the mixture was stirred at room temperature in dark for 10 h. The solvent was evaporated by vacuum. Compound **2** was purified through a silica gel chromatography column as a red solid (0.51 g, 92%). ^{1}H NMR ($CDCl_3$, 300 MHz) δ (ppm): 9.93 (s, 1H, –CHO), 9.85 (s, 1H, –CHO), 7.75–7.69 (m, 2H, ArH), 7.51 (d, *J*=8.4 Hz, 2H, ArH), 7.39–7.29 (m, 4H, ArH), 7.26–7.23 (m, 6H, ArH), 7.04 (d, *J*=8.7 Hz, 2H, ArH), 6.99 (d, *J*=8.4 Hz, 2H, ArH).

2.3.3 5,5'-(4,4'-(4'-*tert*-Butylbiphenyl-4-ylazanediyl)bis-(4,1-phenylene))dithiophene-2-carbaldehyde (**3**)

Compound **2** (0.92 mmol, 0.51 g), 4-*tert*-butylphenylboronic acid (1.5 mmol, 0.25 g), sodium carbonate (10.0 mmol, 1.06 g) were mixed. After carefully degassed and charged with nitrogen, $Pd(PPh_3)_4$ (10 mg) was added, and the solvent of THF and water (2:1) was injected. The reaction was stirred at 80 °C for 24 h and cooled to room temperature. The organic layer was collected, dried over anhydrous sodium sulfate. Compound **3** was purified by column chromatography over silica gel as a dark red solid (0.34 g, 62%). ^{1}H NMR ($CDCl_3$, 300 MHz) δ (ppm): 9.95 (s, 1H, –CHO), 9.86 (s, 1H, –CHO), 7.71 (d, *J*=3.3 Hz, 1H, ArH), 7.55–7.45 (m, 8H, ArH), 7.41–7.31 (m, 4H, ArH), 7.24–7.10 (m, 4H, ArH), 7.04 (d, *J*=8.7 Hz, 2H, ArH), 6.99 (d, *J*=8.4 Hz, 2H, ArH), 1.36 (s, 9H, $–CH_3$).

2.3.4 3,3'-(5,5'-(4,4'-(4'-*tert*-Butylbiphenyl-4-ylazanediyl)-bis(4,1-phenylene))bis(thiophene-5,2-diyl))bis(2-cyanoacrylic acid) (**LI-33**)

Compound **3** (0.33 mmol, 0.20 g) and cyanoacetic acid (1.0 mmol, 0.085 g) were mixed with vacuum-dried, then 15 mL of MeCN, 5 mL of THF and 10 μL of piperidine were added respectively. The solution was stirred at 75 °C for 8 h. Then, the solution was cooled, and the organic layer was evaporated by vacuum. Dye **LI-34** was purified by column chromatography over silica gel as a dark red solid (0.15 g, 67%). m.p.: 193–197 °C. ^{1}H NMR ($CDCl_3$, 300 MHz) δ (ppm): 8.46 (s, 2H, –CH=), 7.97 (br, 2H, ArH), 7.71–7.65 (m, 8H, ArH), 7.54–7.48 (m, 8H, ArH), 7.15–7.03 (m, 4H, ArH), 1.29 (s, 9H, $–CH_3$). ^{13}C NMR (DMSO-d_6, 75 MHz) δ (ppm): 164.9, 164.0, 150.2, 145.7, 144.3, 143.1, 138.3, 137.5, 131.1, 130.4, 128.4, 127.3, 125.4, 123.3, 117.7, 34.7, 31.7. MALDI-TOF MS Calcd. for $C_{44}H_{33}N_3O_4S_2$ [M] *m*/*z*: 731.1912; Found. $C_{44}H_{33}N_3O_4S_2$ (M): 731.1924.

2.3.5 4,4'-(4-Bromophenylazanediyl)dibenzaldehyde (**4**)

After 4,4'-(phenylazanediyl) dibenzaldehyde (6.6 mmol, 2.0 g) was dissolved in $CHCl_3$ (15 mL), *N*-bromosuccinimide (7.4 mmol, 1.3 g) was added slowly. Then, the reaction was stirred at room temperature in dark for 10 h. After that, the solvent was evaporated by vacuum. The product **4** was purified through a silica gel chromatography column as a yellow solid (2.14 g, 85%). ^{1}H NMR ($CDCl_3$, 300 MHz) δ (ppm): 9.91 (s, 2H, –CHO), 7.79 (d, *J*=8.6 Hz, 4H, ArH), 7.50 (d, *J*=8.7 Hz, 2H, ArH), 7.18 (d, *J*=8.6 Hz, 4H, ArH), 7.06 (d, *J*=8.6 Hz, 2H, ArH).

2.3.6 4,4'-(4'-*tert*-Butylbiphenyl-4-ylazanediyl)dibenzaldehyde (**5**)

Compound **4** (1.3 mmol, 0.50 g), 4-*tert*-butylphenyl boronic acid (1.5 mmol, 0.25 g), sodium carbonate (10.0 mmol, 1.06 g) were mixed. After carefully degassed and charged with nitrogen, $Pd(PPh_3)_4$ (10 mg) was added, and the solvent of THF and water (2:1) was injected. The mixture was stirred at 80 °C for 24 h and cooled to room temperature. The organic layer was collected and dried over anhydrous sodium sulfate. Compound **5** was purified by column chromatography over silica gel as a red solid (0.40 g, 70%). ^{1}H NMR ($CDCl_3$, 300 MHz) δ (ppm): 9.91 (s, 2H, –CHO), 7.77 (d, *J*=8.3 Hz, 4H, ArH), 7.51 (br, 4H, ArH), 7.40 (d, *J*=8.5 Hz, 2H, ArH), 7.19 (d, *J*=8.3 Hz, 4H, ArH), 7.09 (d, *J*=8.5 Hz, 2H, ArH), 1.35 (s, 9H, $–CH_3$).

2.3.7 4'-*tert*-Butyl-*N*,*N*-bis(4-((*E*)-2-(thiophen-2-yl)vinyl)-phenyl)biphenyl-4-amine (**6**)

Under an atmosphere of dry nitrogen, diethyl thiophen-2-yl methylphosphonate (2.0 mmol, 0.47 g) was suspended in anhydrous tetrahydrofuran (20 mL), then *t*-BuOK (5.0 mmol, 0.56 g) was added directly as a solid. After that, keep the resultant mixture stirred for 10 min at room temperature. Then, adding the solution of compound **5** (0.92 mmol, 0.4 g) in 20 mL of anhydrous tetrahydrofuran dropwise, the reaction mixture was stirred overnight at room temperature. A

100 mL of water was poured into the mixture to terminate the reaction. The organic product was extracted with $CHCl_3$, and dried over anhydrous sodium sulfate. Compound **6** was purified through a silica gel chromatography column as a yellow solid (0.41 g, 73%). ^{1}H NMR ($CDCl_3$, 300 MHz) δ (ppm): 7.54–7.44 (m, 6H, ArH), 7.38–7.33 (m, 4H, ArH), 7.19–7.09 (m, 8H, ArH), 6.97–6.79 (m, 8H, ArH and –CH=CH–), 1.36 (s, 9H, $-CH_3$).

2.3.8 5,5'-(1*E*,1'*E*)-2,2'-(4,4'-(4'-*tert*-butylbiphenyl-4-ylazanediyl)bis(4,1-phenylene))bis(ethene-2,1-diyl)dithiophene-2-carbaldehyde (**7**)

Under an atmosphere of dry nitrogen, DMF (8.0 mmol, 0.62 mL) was injected into freshly distilled $POCl_3$ (5.0 mmol, 0.74 mL) at zero degree. After it completely transformed into a glassy solid, compound **6** (0.67 mmol, 0.40 g), which dissolved in 20 mL of 1,2-dichloromethane, was added dropwise. The reaction was stirred overnight at room temperature, then poured into an aqueous solution of sodium acetate (1 mol/L, 200 mL), and stirred for another 2 h. The mixture was extracted with $CHCl_3$ for three times, the organic fractions were collected, then dried over anhydrous sodium sulfate. After removing the solvent by vacuum, compound **7** was purified through a silica gel chromatography column as a yellow solid (0.32 g, 73%). ^{1}H NMR ($CDCl_3$, 300 MHz) δ (ppm): 9.85 (s, 2H, –CHO), 7.66 (d, *J*=3.9 Hz, 4H, ArH), 7.54–7.41 (m, 10H, ArH), 7.20–7.12 (m, 10H, ArH and –CH=CH–), 1.37 (s, 9H, $-CH_3$).

2.3.9 3,3'-(5,5'-(1*E*,1'*E*)-2,2'-(4,4'-(4'-*tert*-butylbiphenyl-4-ylazanediyl)bis(4,1-phenylene))bis(ethene-2,1-diyl)bis(thiophene-5,2-diyl))bis(2-cyanoacrylic acid) (**LI-34**)

Compound **7** (0.31 mmol, 0.20 g) and cyanoacetic acid (1.0 mmol, 0.085 g) were mixed with vacuum-dried, then 15 mL of MeCN, 5 mL of THF and 10 μL of piperidine were added respectively. The solution was stirred at 75 °C for 8 h. Then, cooled to room temperature, the organic layer was evaporated by vacuum. Dye **LI-34** was purified by column chromatography over silica gel as a dark red solid (0.15 g, 63%). m.p.: 207–210 °C. ^{1}H NMR ($CDCl_3$, 300 MHz) δ (ppm): 8.39 (s, 2H, –CH=), 7.88 (br, 2H, ArH), 7.62 (br, 4H, ArH), 7.45 (br, 4H, ArH), 7.39 (br, 2H, ArH), 7.24 (br, 2H, ArH), 7.15 (br, 4H, ArH), 7.01 (br, 6H, ArH and –CH=CH–), 1.31 (s, 9H, $-CH_3$). ^{13}C NMR (DMSO-d_6, 75 MHz) δ (ppm): 165.9, 164.1, 151.7, 150.3, 147.6, 146.8, 145.5, 140.52, 137.5, 134.6, 132.2, 131.1, 130.2, 128.7, 127.2, 127.6, 125.5, 125.9, 124.7, 123.7, 120.1, 117.7, 34.8, 31.7. MALDI-TOF MS Calcd. for $C_{48}H_{37}N_3O_4S_2$ [M] *m/z*: 783.2225; Found, $C_{48}H_{37}N_3O_4S_2$ (M): 783.2234.

2.4 Device fabrication

The DSSCs based on these two dyes were fabricated similarly with the literature [16].

3 Results and discussion

3.1 Synthesis of the sensitizers

The synthetic procedure was shown in Scheme 1. As to **LI-33**, after the normal Suzuki coupling reaction between the bromine exposed intermediate and 5-formylthiophen-2-ylboronic acid, compound **2** was obtained easily. Then, 4-*tert*-butylbenzene moiety was introduced to the donor side of the molecule via Suzuki reaction. For **LI-34**, **5** was brominated by *N*-bromosuccinimide (NBS), then a Suzuki reaction of **5** produced the corresponding compound **6**, which underwent another Wittig reaction with diethyl thio phen-2-ylmethyl phosphonate to yield compound **7**. Dialdehyde **8** was obtained by the following Vilsmeier reaction. Finally, two organic dyes were produced through the Knoevenagel condensation reactions in the presence of piperidinen, and from **4** and **8** with cyanoacetic acid. All the intermediates and two target organic sensitizers were confirmed by ^{1}H and ^{13}C NMR, and MALDI-TOF-MS.

3.2 Absorption spectra

The absorption spectra of dyes in dichloromethane solution were displayed in Figure 1 and the corresponding data were collected in Table 1. There are two distinct absorptions around 340 and 500 nm. Generally, the π-π* transitions of the dyes could lead to the absorption band around 340 nm, while an intramolecular charge transfer (ICT) along the whole molecules resulted in the absorption band around 500 nm. In comparison with **LI-33**, the absorption maximum of **LI-34** (511 nm) red shifted 41 nm, indicating that a vinyl thiophene unit instead of thiophene, can be beneficial to the conjugation of whole molecule. And in contrast to conventional ruthenium complexes (for example, 13900 L/(mol cm) at 541 nm for **N3**), the present dye molecules show about

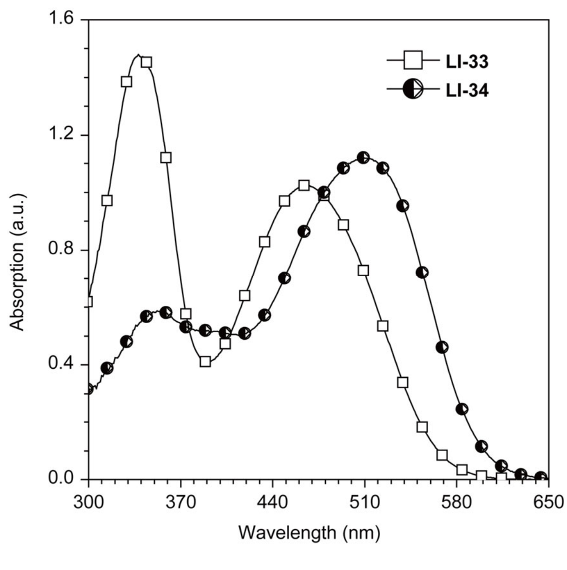

Figure 1 UV-Vis spectra of dyes in CH_2Cl_2.

Table 1 Absorbance and electrochemical properties of dyes

Dye	λ_{max} [a)] (nm)	ε [a)] (L/(mol cm))	λ_{max} [b)] (nm)	$E_{0\text{-}0}$ [c)] (eV)	E_p [d)] (V)	E_{ox} [e)] (V) vs. NHE	E_{red} [f)] (V) vs. NHE
LI-33	470	42500	476	2.18	1.02	1.22	−0.96
LI-34	511	37300	520	2.07	0.87	1.07	−1.20

a) Absorption spectra of dyes measured in CH_2Cl_2 with the concentration of 3×10^{-5} mol/L; b) absorption spectra of dyes adsorbed on the surface of TiO_2; c) the bandgap, $E_{0\text{-}0}$ was derived from the observed optical edge; d) E_p is the peak of DPV (the DPV of the dyes were measured in CH_2Cl_2 with 0.1 mol/L $(n\text{-}C_4H_9)_4NPF_6$ as electrolyte (scanning rate, 100 mV/s; working electrode and counter electrode, Pt wires; reference electrode, Ag/AgCl)); e) the oxidation potential (E_{ox}) referenced to calibrated Ag/AgCl was converted to the NHE reference scale: $E_{ox}=E_p+0.197$ V; f) E_{red} was calculated from $E_{ox}-E_{0\text{-}0}$.

three times of absorption coefficients, 42500 L/(mol cm) for **LI-33** and 37300 L/(mol cm) for **LI-34**, respectively, suggesting that the two dyes can harvest the sun-light efficiently.

The absorption spectra of organic sensitizers on the TiO_2 film (6 μm) were shown in Figure 2. The absorption maxima of the two dyes were located at 476 and 520 nm, which red-shifted by 6 and 9 nm than those in the solution, respectively, hinting that the aggregates of two dyes on the TiO_2 surface was not severe. This well-organized arrangement may be ascribed to the introduction of 4-*tert*-butylbenzene moiety on the donor part, which can reduce the intermolecular coupling and π-π stacking. Similar to the absorption in solution, **LI-34** exhibited significant broader absorption in the visible region than that of **LI-33**, and extended the absorption onset to longer wavelength (λ>700 nm), which would be beneficial to the light harvesting, thus, leading to the increase of J_{sc}.

3.3 Electrochemical properties

Differential pulse voltammetric (DPV) was used to determine the oxidation potential of the two dyes from the peak potentials (E_p) (Figure 3). The highest occupied molecular orbital (HOMO) was derived from the oxidation potential vs. NHE (E_{ox}), while the lowest unoccupied molecular orbital (LUMO) was derived from the reduction potential vs. NHE (E_{red}), which could be calculated from $E_{ox}-E_{0\text{-}0}$. The electrochemical properties of the two dyes were summarized in Table 1. The potential energy of ionization of **LI-33** and **LI-34** were not very close, as a result of their different levels of conjugation. As described in Figure 4, comparing to the iodine/iodide redox potential value (0.4 V vs. NHE), the HOMO levels of the two organic dyes were more positive, indicating that the reduced species in the electrolyte could regenerate the oxidized dyes. It is essential to the operation of the corresponding solar cells. By estimated from the values of E_{ox} and the $E_{0\text{-}0}$ band gaps, the LUMO levels of the dyes were obtained, which were sufficiently negative than the conduction-band-edge energy level (E_{CB}) of the TiO_2 electrode (−0.5 V vs. NHE), suggesting that the excited dye can inject electron into the conduction band of TiO_2 energetically.

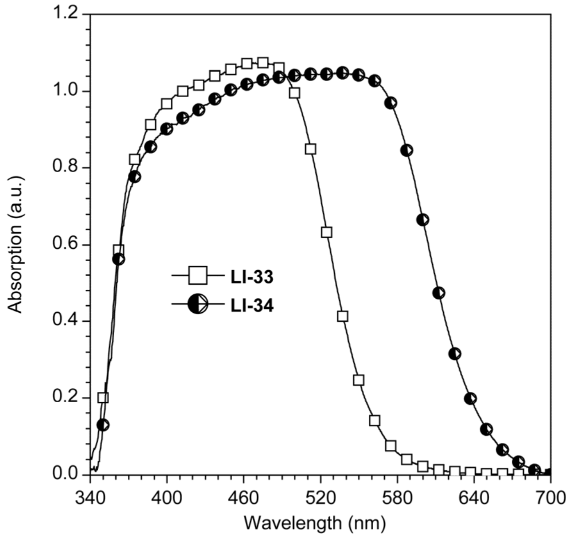

Figure 2 UV-Vis spectra of the dyes on TiO_2 films.

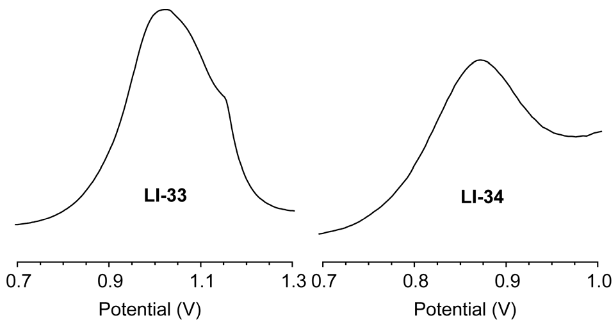

Figure 3 DPV of dyes.

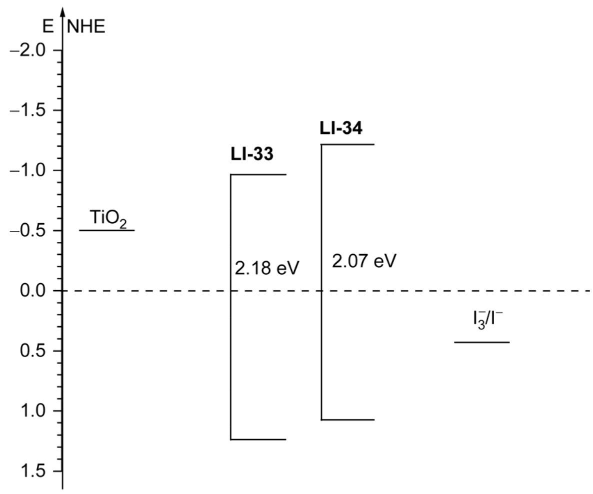

Figure 4 Schematic representation of the band positions in DSSCs based on **LI-33** and **LI-34**.

3.4 Theoretical approach

Quantum chemistry computation was conducted, in order to gain further insight in the correlation between structure and the physical properties as well as the device performance. Time-depending DFT (TDDFT) calculations with Gaussian 09 program was used to optimize the sensitizers geometries and the structures of the sensitizers were analyzed by the B3LYP exchange-correlation functional and a 6-31G* basis set [23]. The electron distributions of the HOMO and LUMO of **LI-33** and **LI-34** were shown in Figure 5.

Similar HOMO/LUMO electron distributions for the two dyes were seen from molecular orbital calculations. The electron density distribution of the HOMO is mainly located at delocalized π orbitals on spacer unit, with the greatest density on the donor part, while the LUMO is primarily localized on the acceptor part. Thus, when the light irradiates to the dyes, the electron could move through the whole molecules to the anchoring moieties. The optimized structures of the two dyes were also depicted in Figure 5. It revealed that the conjugation system of the dyes were nearly planar. However, the 4-*tert*-butylbenzene moieties, which were linked to the electron donor group, were twisted largely. They were just like an umbrella, which suppress the charge recombination and π-π stacking of the dyes.

3.5 Photovoltaic performance of DSSCs

The IPCEs of dyes (Figure 6) were obtained with a sandwich cell using 1,2-dimethyl-3-propylimidazolium iodide (0.6 mol/L), LiI (0.1 mol/L), I_2 (0.05 mol/L), and 4-*tert*-butylpyridine (0.5 mol/L) in acetonitrile and methoxypropionitrile (7:3). The IPCEs of the dyes illustrate that the visible light can be converted to photocurrent efficiently in the region from 400 to 600 nm, in good accordance with their absorption spectra on the TiO_2 film. The IPCE spectrum for **LI-34** exceeded 50% from 350 to 570 nm where the incident photon to current conversion efficiency reached 60% at 473 nm. However, the IPCE values were relatively lower for the solar cells based on **LI-33**, the maximum was only 14%. In order to optimize their photovoltaic performance, the function of co-adsorbents was investigated. As the most popular co-adsorbent, chenodeoxycholic acid (CDCA) would attach to nanostructured TiO_2 strongly, thus, it can displace dye molecules with weak adsorption from the surface of semiconductor TiO_2, which was beneficial to the alignment of dyes on the TiO_2 surface. For comparison, the IPCEs of solar cells, in which TiO_2 film exposed to dye individually, and the ones exposed to 10 mmol/L CDCA before the dye bath were shown in Figure 6. It is certain that the IPCE spectra of the two dyes became broaden after the addition of CDCA, which extended to 700 nm. This broad absorption would favor the light harvesting, resulting in the enhancement of J_{sc}. However, the effect of CDCA on the IPCE values of the two dyes was different. For **LI-34**, the IPCE values changed little, indicating that the degree of the dye aggregations on the TiO_2 surface was not very much, which should be attributed to the introduction of the *tert*-butyl group. The steric and nonplanar structure of the *tert*-butyl group in **LI-34** could help to suppress the dye aggregates and electron recombination [24,25]. However, for **LI-33**, the maximum value of the IPCE spectra increased much more after the addition of 10 mmol/L CDCA, from 14% to 35%, meaning that the introduction of CDCA can favor the well-organized arrangement of **LI-33** on the TiO_2 surface or help them be absorbed on the TiO_2 film efficiently.

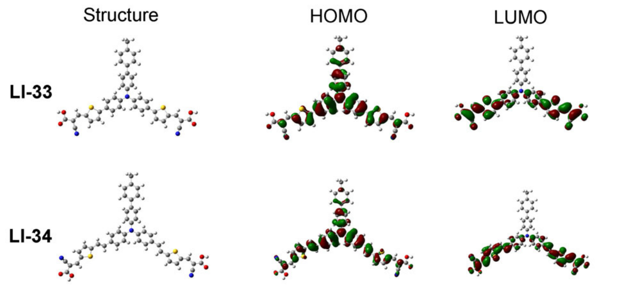

Figure 5 Frontier orbitals of the dyes **LI-33** and **LI-34** optimized at the B3LYP/6-31+G (D) level.

Figure 7 showed the photocurrent-voltage (*J-V*) plots of DSSCs fabricated with these dyes under AM 1.5G simulated sunlight at 100 mW/cm^2, and the photovoltaic characteristic parameters, including short circuit current (J_{sc}), open-circuit photovoltage (V_{oc}), fill factor (*FF*), and solar-to-electrical photocurrent density (η) were summarized in Table 2, where **N719** is included for comparison. For the extended conjugated system, **LI-34** gave the better performance with J_{sc} of 14.95 mA/cm^2, V_{oc} of 0.64 V and *FF* of 0.59, leading to a η value of 5.61%, which further confirm the superiority of vinyl thiophene uint as the conjugated bridge. The much lower conversion efficiency of **LI-33** (1.89%) may be due to its shorter conjugated bridge, which makes the two anchoring groups much close to each other, thus, the interaction of them would adverse to the adsorption of the dyes on TiO_2 surface, resulting in the poorer light harvesting, then to the lower values of J_{sc} and η. This phenomenon was consistent with the IPCE spectra. With the aim to further optimize their photovoltaic properties, the function of CDCA was also considered. After the addition of CDCA, the conversion efficiencies of the two dyes increased. As to dye **LI-33**, J_{sc} values increased from 4.7 to 8.8 mA/cm^2, and the η value reached 3.41%. DSSC based on **LI-34** with 10 mmol/L CDCA showed the highest solar to electricity conversion efficiency of 6.05% (J_{sc}=14.61 mA/cm^2, V_{oc}=0.67 V, *FF*=0.62) among these devices, which reached 86% of a **N719**-based DSSC (7.83%), which was fabricated and measured under the same conditions.

4 Conclusions

Two new dye sensitizers **LI-33** and **LI-34**, were synthesized, which contain 4-*tert*-butylbenzene substituted TPA as

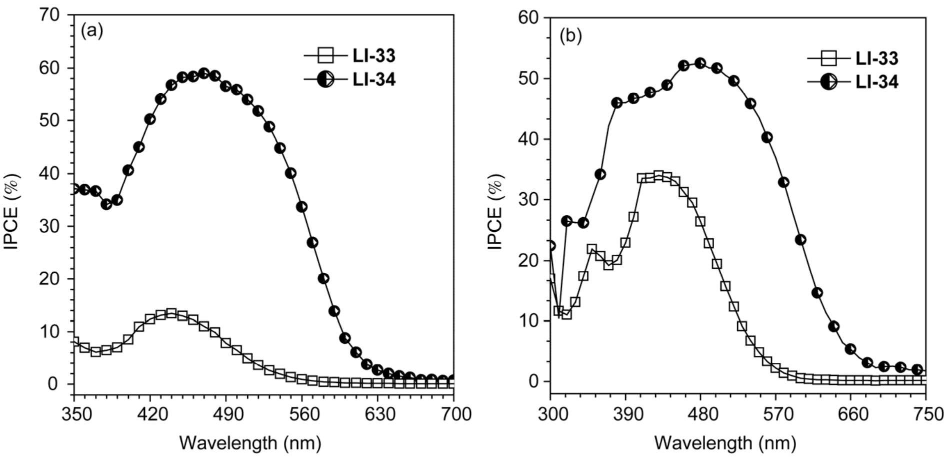

Figure 6 Spectra of monochromatic incident photon-to-current conversion efficiency (IPCE) for DSSCs based on **LI-33** and **LI-34**. (a) Without CDCA; (b) with 10 mmol/L CDCA.

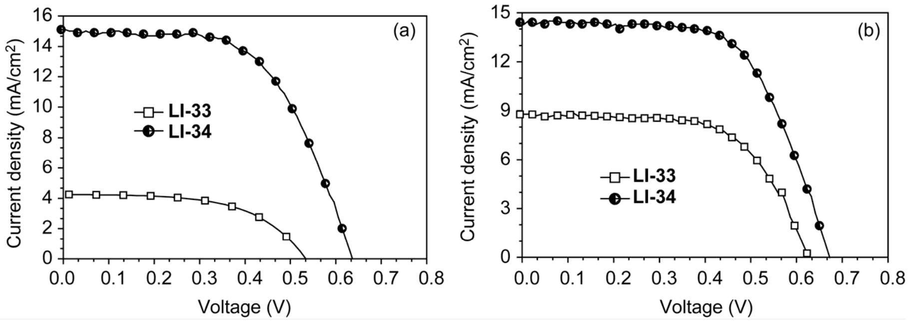

Figure 7 Current density-voltage characteristics obtained with a nanocrystalline TiO_2 film supported on FTO conducting glass and derivatized with monolayer of the sensitizers. (a) Without CDCA; (b) with 10 mmol/L CDCA.

Table 2 DSSCs performance data of new dyes [a)]

Dye	CDCA	J_{sc} (mA/cm^2)	V_{oc} (V)	*FF*	η (%)
LI-33	none	4.7	0.54	0.61	1.89
	10 mmol/L	8.8	0.63	0.62	3.41
LI-34	none	14.95	0.64	0.59	5.61
	10 mmol/L	14.61	0.67	0.62	6.05
N719		16.96	0.76	0.61	7.83

a) Illumination: 100 mW/cm^2 simulated AM 1.5 G solar light; electrolyte containing: 0.1 mol/L LiI+0.05 mol/L I_2+0.6 mol/L DMPII+0.5 mol/L TBP in the mixed solvent of acetonitrile and 3-methoxypropionitrile (7:3, *v*/*v*).

the electron donor unit, two cyanoacetic acid units as the electron acceptor part, and thiophene or vinyl thiophene group as the π-bridge. Two acceptor units were designed to create multiple channels for the electron injection into TiO_2 electrode to enhance the efficiency of DSSCs. DSSCs based on **LI-34** with 10 mmol/L CDCA showed the best light to electricity conversion efficiency of 6.05% (J_{sc}=14.61 mA/cm^2, V_{oc}=0.67 V, *FF*=0.62). The preliminary results demonstrated that the introduction of two acceptor units may be able to increase the efficiency of DSSCs, and more follow-up work is underway in our laboratory.

This work was supported by the National Natural Science Foundation of China (21372003, 21325416), and the National Basic Research Program of China (2011CB932702).

1 Armaroli N, Balzani V. The future of energy supply: challenges and opportunities. *Angew Chem Int Ed*, 2007, 46: 52–66
2 Listorti A, O'Regan B, Durrant JR. Electron transfer dynamics in dye-sensitized solar cells. *Chem Mater*, 2011, 23: 3381–3399
3 Hagfeldt A, Boschloo G, Sun L, Kloo L, Pettersson H. Dye-sensitized solar cells. *Chem Rev*, 2010, 110: 6595–6663
4 O'Regan B, Grätzel M. A low-cost, high-efficiency solar cell based on dye-sensitized colloidal TiO_2 films. *Nature*, 1991, 353: 737–740
5 Ning Z, Tian, H. Triarylamine: a promising core unit for efficient photovoltaic materials. *Chem Commun*, 2009, 45: 5483–5495
6 Yum JH, Baranoff E, Wenger S, Nazeeruddin MK, Grätzel M. Panchromatic engineering for dye-sensitized solar cells. *Energy Environ Sci*, 2011, 4: 842–857
7 Calogero G, Di Marco G, Cazzanti S, Caramori S, Argazzi R, Bignozzi CA. Natural dye senstizers for photoelectrochemical cells *Energy Environ Sci*, 2009, 2: 1162–1172
8 Ooyama Y, Harima Y. Molecular designs and syntheses of organic dyes for dye-sensitized solar cells. *Eur J Org Chem*, 2009, 18: 2903–2934
9 Li Q, Lu L, Zhong C, Huang J, Huang Q, Shi J, Jin X, Peng T, Qin J, Li Z. New pyrrole-based organic dyes for dye-sensitized solar cells: convenient syntheses and high efficiency. *Chem Eur J*, 2009, 15: 9664–9668
10 Li Q, Lu L, Zhong C, Huang Q, Shi J, Jin X, Peng T, Qin J, Li Z.

New indole-based metal-free organic dyes for dye-sensitized solar cells. *J Phys Chem B*, 2009, 113: 14588–14595

11 Liu B, Zhu W, Zhang Q, Wu W, Xu M, Ning Z, Xie Y, Tian H. Conveniently synthesized isophoronedyes for high efficiency dye-sensitized solar cells: tuning photovoltaic performance by structural modification of donor group in donor-π-acceptor system. *Chem Commun*, 2009, 45: 1766–1768

12 Shi J, Chai Z, Zhong C, Wu W, Hua J, Dong Y, Qin J, Li Q, Li Z. New efficient dyes containing *tert*-butyl in donor for dye-sensitized solar cells. *Dyes Pigm*, 2012, 95: 244–251

13 Li Q, Shi J, Li H, Li S, Zhong C, Guo F, Peng M, Hua J, Qin J, Li Z. Novel pyrrole-based dyes for dye-sensitized solar cells: from rod-shape to "H" type. *J Mater Chem*, 2012, 22: 6689–6696

14 Lu M, Liang M, Han H, Sun Z, Xue S. Organic dyes incorporating bis-hexapropyltruxeneamino moiety for efficient dye-sensitized solar cells. *J Phys Chem C*, 2011, 115: 274–281

15 Zhu W, Wu Y, Wang S, Li W, Li X, Chen J, Wang Z, Tian H. Organic D-A-π-A solar cell sensitizers with improved stability and spectral response. *Adv Funct Mater*, 2011, 21: 756–763

16 Shi J, Huang J, Tang R, Chai Z, Hua J, Qin J, Li Q, Li Z. Efficient metal-free organic sensitizers containing tetraphenylethylene moieties in the donor part for dye-sensitized solar cells. *Eur J Org Chem*, 2012, 27: 5248–5255

17 Shi J, Chen J, Chai Z, Wang H, Tang R, Fan K, Wu M, Han H, Qin J, Peng T, Li Q, Li Z. High performance organic sensitizers based on 11,12-bis(hexyloxy) dibenzo[*a*,*c*]phenazine for dye-sensitized solar cells. *J Mater Chem*, 2012, 22: 18830–18838

18 Shi J, Chai Z, Su J, Chen J, Tang R, Fan K, Zhang L, Han H, Qin J, Peng T, Li Q, Li Z. New sensitizers bearing quinoxaline moieties as an auxiliary acceptor for dye-sensitized solar cells. *Dyes Pigm*, 2013, 98: 405–413

19 Ning Z, Fu Y, Tian H. Improvement of dye-sensitized solar cells: what we know and what we need to know. *Energy Environ Sci*, 2010, 3: 1170–1181

20 Abbotto A, Manfredi N, Marinzi C, De Angelis F, Mosconi E, Yum JH, Zhang X, Nazeeruddin MK, Grätzel M. Di-branched di-anchoring organic dyes for dye-sensitized solar cells. *Energy Environ Sci*, 2009, 2: 1094–1101

21 Shi L, He C, Zhu D, He Q, Li Y, Chen Y, Sun Y, Fu Y, Wen D, Cao H, Cheng J. High performance aniline vapor detection based on multi-branched fluorescent triphenylamine-benzothiadiazole derivatives: branch effect and aggregation control of the sensing performance. *J Mater Chem*, 2012, 22: 11629–11635

22 Goswami S, Manna A, Paul S, Aich K, Das AK, Chakraborty S. Highly reactive (<1 min) ratiometric probe for selective "naked-eye" detection of cyanide in aqueous media. *Tetrahedron Lett*, 2013, 54: 1785–1789

23 Frisch MJ, Trucks GW, Schlegel HB, Scuseria GE, Robb MA, Cheeseman JR, Scalmani G, Barone V, Mennucci B, Petersson GA, Nakatsuji H, Caricato M, Li X, Hratchian HP, Izmaylov AF, Bloino J, Zheng G, Sonnenberg JL, Hada M, Ehara M, Toyota K, Fukuda R, Hasegawa J, Ishida M, Nakajima T, Honda Y, Kitao O, Nakai H, Vreven T, Montgomery Jr JA, Peralta JE, Ogliaro F, Bearpark M, Heyd JJ, Brothers E, Kudin KN, Staroverov VN, Kobayashi R, Normand J, Raghavachari K, Rendell A, Burant JC, Iyengar SS, Tomasi J, Cossi M, Rega N, Millam JM, Klene M, Knox JE, Cros JB, Bakken V, Adamo C, Jaramillo J, Gomperts R, Stratmann RE, Yazyev O, Austin AJ, Cammi R, Pomelli C, Ochterski JW, Martin RL, Morokuma K, Zakrzewski VG, Voth GA, Salvador P, Dannenberg JJ, Dapprich S, Daniels AD, Farkas Ö, Foresman JB, Ortiz JV, Cioslowski J, Fox DJ. Gaussian 09. Wallingford CT: Gaussian, Inc., 2009

24 Koumura N, Wang Z, Mori S, Miyashita M, Suzuki E, Hara K. Alkyl-functionalized organic dyes for efficient molecular photovoltaics. *J Am Chem Soc*, 2006, 128: 14256–14257

25 Miyashita M, Sunahara K, Nishikawa T, Uemura YN, Hara K, Mori A, Abe T, Suzuki E, Mori S. Interfacial electron-transfer kinetics in metal-free organic dye-sensitized solar cells: combined effects of molecular structure of dyes and electrolytes. *J Am Chem Soc,* 2008, 130: 17874–17881